Charge-Transfer and Thermochromic Phenomena in Solid Polyelectrolytes

J. S. Moore and S. I. Stupp*

Polymer Group, College of Engineering, University of Illinois at Urbana-Champaign, Urbana, Illinois 61801. *Received November 21, 1985*

ABSTRACT: Aromatic polyelectrolytes capable of undergoing charge-transfer interactions with their counterions were synthesized and studied in the solid state by several physical techniques. The polyelectrolytes were formed by the condensation of 4,4′-bipyridine with aromatic dihalides yielding polycations with quaternary nitrogens in the repeating unit. The work focused on the polyelectrolyte known as poly(xylylviologen dibromide) (PXV-Br_2) but other polymeric and monomeric chemical analogues were prepared and analyzed as part of the study. Visible light absorption of PXV-Br_2 was characterized by diffuse reflectance measurements as a function of temperature and degree of hydration in the polyelectrolyte. We found a reversible thermochromic effect consisting of a visible bathochromic shift as PXV-Br_2 is heated above 100 °C. Through thermogravimetric analysis and other experiments, the shift was attributed to the level of surface hydration, presumably as a result of how water molecules bound to the macroion affect charge-transfer states. A study of polymerization kinetics in PXV-Br_2 by infrared spectroscopy suggests that water molecules are closely associated with the cationic repeating units. Consideration of recent theoretical work and experimental results suggests that the phenomenon of counterion condensation and the presence of amorphous regions contribute to strong charge-transfer interactions in these polyelectrolytic solids.

Introduction

An important area of contemporary polymer science is the study of macromolecules exhibiting a highly specific physical response to external stimuli or to subtle changes in their environment. The most sophisticated and complex examples of such polymers are found in biological systems, but fundamental studies on this subject require the use of simpler macromolecules. We report here our studies on a family of chromatically active polyelectrolytes, which we found to be highly sensitive to molecular environment.

An example of macromolecules with inherent chromatic properties is the poly(diacetylenes). The wavelength of visible light absorption in these polymers depends on degree of polymerization, molecular structure, solvent, temperature, and the nature of the solid phase.[1,2] Other examples are the poly(bisthiophenes), which exhibit electrochromic behavior,[3] and the group of ionenes[4,5] studied in the present work known as poly(xylyl viologens) (PXV's).[6-11] The general structure of these polyelectrolytes is shown here.

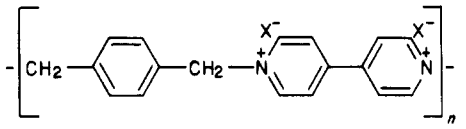

$X^- = Cl^-, Br^-, I^-$

The bipyridinium moiety present in the backbone of PXV's is known to exhibit chromatic activity, presumably as a result of charge-transfer complexation.[12,13] The sensitivity of charge-transfer energy levels in these polymers to structural features and molecular environment is one factor that remains unclear at the present time. Structural features that may be important include repeating-unit chemistry as well as macromolecular and Coulombic structure. Coulombic structure would include the distribution of condensed vs. loosely bound counterions in the solid polyelectrolyte. This paper addresses such issues in the bipyridinium polyelectrolytes, with special emphasis on the interactions of the macroion with water and counterions. The thermochromic behavior of these solid polyelectrolytes has been studied as well. The investigation included macroion synthesis followed by experiments with techniques such as visible reflectance spectroscopy, thermogravimetric analysis (TGA), X-ray diffraction, and infrared spectroscopy.

Experimental Section

Synthesis. The names, abbreviations, and chemical structures of polyelectrolytes and monomeric model compounds studied in this investigation are shown in Table I. The starting materials, 4,4′-bipyridine, α,α′-*p*-dibromoxylene, α,α′-*p*-dichloroxylene, 1,2-bis(4-pyridyl)ethane, and 1,2-bis(4-pyridyl)ethylene, were supplied by Aldrich Chemical Co. 4,4′-Bipyridine was obtained as the dihydrate with the melting range 71–75 °C. In order to remove the hydration water this compound was heated to 150 °C under a vacuum of 25 mm Hg for 2 h and then recrystallized from carbon tetrachloride (mp 110–112 °C). α,α′-*p*-Dibromoxylene and α,α′-*p*-dichloroxylene were recrystallized from *p*-dioxane and 1,2-bis(4-pyridyl)ethylene and 1,2-bis(4-pyridyl)ethane from distilled water. All four compounds were vacuum dried overnight after recrystallization. α,α′-*p*-Diiodoxylene was prepared from α,α′-*p*-dichloroxylene and sodium iodide in acetone by the Finkelstein reaction using the following procedure. A mixture of 9.96 g of dichloroxylene and 25.6 g of sodium iodide in 35 mL of acetone was refluxed overnight. The solvent was removed under vacuum and the residue extracted with chloroform and water. The organic layer was dried over $MgSO_4$ and filtered, and the solvent was removed under vacuum. The residue was recrystallized from *p*-dioxane and vacuum dried overnight: mp 177–179 °C [lit.[14] mp 179.5–180 °C]. All other reagents and solvents were used without further purification.

Pyridinium ionene polymers used in solid-state reflectance studies were synthesized from anhydrous bipyridine and the corresponding dihaloxylene by the Menschutkin reaction. PXV-Cl_2 was synthesized by mixing 1.952 g (0.0125 mol) of anhydrous 4,4′-bipyridine and 2.188 g (0.0125 mol) of α,α′-*p*-dichloroxylene in 25 mL of acetonitrile. This clear solution was stirred in a tightly sealed flask at room temperature for about 8 days. Similarly, PXV-Br_2 was formed by reacting 1.952 g (0.0125 mol) of the purified bipyridine and 3.300 g (0.0125 mol) of α,α′-*p*-dibromoxylene in 25 mL of acetonitrile at room temperature for about 4 days. PXV-I_2 was synthesized from 1.952 g (0.0125 mol) of anhydrous bipyridine and 4.474 g (0.0125 mol) of α,α′-*p*-diiodoxylene at room temperature in 25 mL of acetonitrile mixed over the course of about 4 days. PXPV-Br_2 was prepared by reacting 2.625 g (0.0125 mol) of 1,2-bis(4-pyridyl)ethylene, 3.300 g (0.0125 mol) of α,α′-*p*-dibromoxylene and 25 mL of acetonitrile at room temperature for 3 days. PXPE-Br_2 was produced by mixing 2.650 g (0.0125 mol) of 1,2-bis(4-pyridyl)ethane and 3.300 g (0.0125 mol) of α,α′-*p*-dibromoxylene in 25 mL of acetonitrile at ambient temperature over a period of 5 days. Poly(*n*-butylviologen) was prepared by combining 2.352 g of 4,4′-bipyridine

0024-9297/86/2219-1815$01.50/0

Table I

chemical structure	counterion (X^-)	symbol
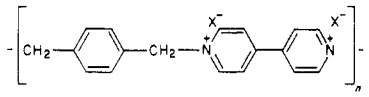	Cl^- Br^- I^-	PXV-Cl_2 PXV-Br_2 PXV-I_2
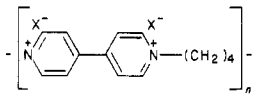	Br^-	PBV-Br_2
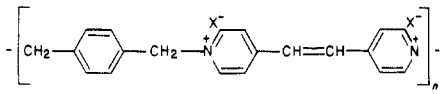	Br^-	PXPV-Br_2
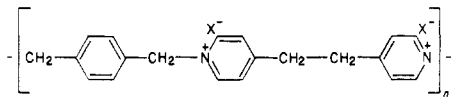	Br^-	PXPE-Br_2
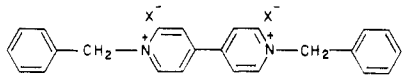	Br^-	DBV-Br_2

and 3.237 g of 1,4-dibromobutane in 30 mL of acetonitrile at 25 °C. The solution was stirred for 3 days. The model compound, DBV-Br_2, was synthesized by combining 1.952 g (0.0125 mol) of 4,4′-bipyridine in 25 mL of acetonitrile with a large excess of benzyl bromide. In all reactions described above, the precipitated material was collected by suction filtration and washed with two 25-mL portions of chloroform. The solids collected were ground in a mortar until a fine, uniform consistency was reached and then dried under a vacuum of about 1.0 mmHg at room temperature for 24 h. The solid samples were stored in a desiccator until their reflectance spectra were recorded.

For the study of the effect of hydration on chromatic behavior, 0.976 g (0.00625 mol) of anhydrous 4,4′-bipyridine were weighed into a 25-mL volumetric flask. This flask was then filled with enough *p*-dioxane to completely dissolve the bipyridine. The desired amount of distilled water was then accurately measured into a 25-mL volumetric flask and *p*-dioxane was added to the mark. The contents of the volumetric flask were poured into a 50-mL round-bottom flask that contained 1.650 g (0.00625 mol) of α,α'-*p*-dibromoxylene. The flask was then sealed tightly and stirred at room temperature.

A polyelectrolyte complex of PXV-Br_2 and ionized poly(acrylic acid) was prepared by mixing 2.342 g of 4,4′-bipyridine and 3.959 g of α,α'-*p*-dibromoxylene in 60 mL of dioxane. To this mixture was added 30 mL of a 3.4 wt % solution of poly(acrylic acid) ionized 20% with sodium hydroxide. The resulting suspension was stirred for 6 days, yielding a thick yellow paste.

Physical Measurements. Ultraviolet–visible spectra of ionene polymer solutions were recorded on a Perkin-Elmer 55B spectrophotometer. Diffuse reflectance data of powders and slurries were recorded with a Beckman DK-2A spectroreflectometer. This instrument resembles a typical double-beam photometer except that monochromatic radiation enters an integrating sphere rather than passing through a sample cell. Radiation entering the sphere is alternately directed toward the sample and the reference. The sphere acts to collimate scattered radiation from the samples and reference into the detector. The spectroreflectometer used in this investigation ratios the sample reflectance against the reflectance of some reference material. In normal operation, the reference is a white substance such as $BaSO_4$ with high reflecting power over the region of interest. For materials whose reflectance spectra are nearly identical, however, it is possible to elucidate small differences in their chromaticity by placing one of these materials in the sample compartment and the other in the reference compartment. In this manner, the reflectance ratio of the two materials can be easily recorded. Powder samples for diffuse reflectance were packed into the sample holder with a Bausch and Lomb powder press. Unless otherwise indicated, reflectance spectra were recorded relative to a barium sulfate standard. Reflectance measurements to study chromaticity vs. hydration were carried out on slurries obtained directly from the vessels of synthetic reactions. This method was necessary in order to minimize exposure of the hygroscopic materials to atmospheric moisture. A special cell supplied by Beckman Instruments was used to hold the slurry samples.

In order to monitor thermochromic activity, a sample cell was constructed in our laboratory containing both a heating element and a thermocouple. The heating element was constructed from Chromel wire coiled around the face of the back plate and cemented in place with an epoxy resin. The temperature was controlled by a voltage regulator and monitored with a Chromel–Alumel thermocouple positioned in a small hole through the back plate such that it made contact with the sample. X-ray scans were recorded on a Philips diffractometer, using Cu Kα radiation. Thermogravimetric analysis (TGA) data was obtained on a Du Pont thermal analyzer equipped with a TGA cell. Sample weight loss was monitored upon heating in the TGA cell under an atmosphere of dry nitrogen at a heating rate of 10 °C/min. Readsorption of water was induced through exposure of the cell to the atmosphere. Changes in the material's color with water readsorption were monitored through a series of timed photographs after the TGA cell was opened.

Polymerization Kinetics. The reaction's progress was monitored by transmission infrared spectroscopy. Deuterium oxide was used instead of H_2O since the latter absorbs strongly at 1640 cm^{-1} and this interferes with measurements of extent of reaction (the infrared absorption of D_2O is small in the range 1660–1570 cm^{-1}). Polymerization kinetics were studied at a 0.250 M concentration for each monomer at a temperature of 24 ± 2 °C. 0.976 g (0.00625 mol) of bipyridine were weighed into a 25-mL volumetric flask. Enough freshly opened *p*-dioxane was added to completely dissolve the bipyridine. Next, the appropriate amount of D_2O was carefully weighed into the flask, which was then filled to the mark with *p*-dioxane. Next, 1.650 g (0.00625 mol)e of α,α'-*p*-dibromoxylene were placed in a 50-mL round-bottom flask containing a magnetic stirrer. The reaction was started by emptying the contents of the volumetric flask into the round-bottom flask. At this point, the reaction flask was tightly stoppered in order to prevent permeation of atmospheric moisture. At the appropriate time the flask was opened to remove a sample of the reaction mixture for infrared analysis and rapidly resealed. A small quantity of this slurry (1–2 drops) was placed directly between two NaCl plates and the infrared spectrum recorded in the range 1680–1550 cm^{-1} with a Beckman 4240 spectrometer. This process was repeated 4 times for each sample removed from the reaction flask. The data were obtained as percent transmittance and converted to absorbance. Reaction progress was followed over a period of 56 h with readings every 4 h for the first 22 h, and then every 8 h for the remainder of the experimental period.

Results and Discussion

All but one of the pyridinium polymers synthesized were brightly colored, as indicated in Table II. In all cases,

Table II
Optical Properties of Experimental Polyelectrolytes

polyelectrolyte	λ_{max}, nm	$F(R'_\infty)_{max}$	color
PXV-Cl_2	<350		green-blue
PXV-Br_2	405	4.8	yellow
PXV-I_2	480	10.2	orange-red
PXPE-Br_2	<350		white
PXPV-Br_2	400	5.3	yellow

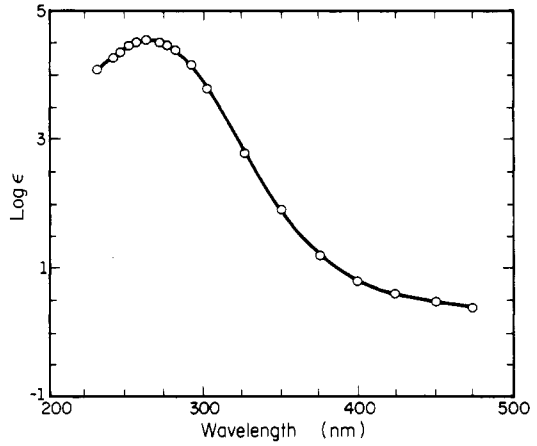

Figure 1. Log plot of extinction coefficient, ϵ, vs. wavelength in the ultraviolet–visible range of an aqueous solution of PXV-Br_2.

however, the final chromatic state was preceded by a white or faintly colored precipitate in the very early stages of polymerization. The chromaticity of these precipitates was found to intensify with reaction time. The rate of color change was observed to depend strongly on the polymerization solvent, specifically on the concentration of water in the reaction medium (a detailed study of the effect of water on polymerization kinetics is discussed elsewhere in the paper). All the polyelectrolytes synthesized for this work were slightly soluble in water, and the aqueous solutions were only faintly colored relative to the solid state. This is clearly revealed in Figure 1 by a log plot of extinction coefficient, ϵ, for an aqueous solution of PXV-Br_2. The solution exhibits a strong absorption in the UV range, but it is only weakly absorbing in the range of visible wavelengths.

Diffuse reflectance spectroscopy was used to quantify the chromaticity of the polyelectrolytes in the solid state. The spectroreflectometer used in this study records the ratio of percent reflectance as a function of wavelength. Percent reflectance is defined from the ratio of light reflected by the sample to light reflected by the standard. From the diffuse reflectance theory of Kubelka and Munk,[15] it is possible to transform this data into a spectrum that resembles the absorption curve of the material. With eq 1, the reflectance value at a given wavelength is

$$F(R'_\infty) = (1 - R'_\infty)^2/2R'_\infty = \kappa/S \qquad (1)$$

converted to its value of the remission function, $F(R'_\infty)$, where R'_∞ is the ratio of diffuse reflectance of the sample to that of the standard, κ represents the absorption coefficient, and S is the scattering coefficient. Under conditions where particle size is much larger than wavelength, it has been shown that S becomes essentially independent of wavelength. Therefore, changes in $F(R'_\infty)$ with wavelength are directly proportional to changes in the material's absorption coefficient with wavelength. The result of the transformation of data from R'_∞ to $F(R'_\infty)$ has been illustrated in Figure 2, where we have plotted $F(R'_\infty)$ for PXV-Br_2, PXV-I_2 and PXV-Cl_2. Comparison of Figures 1 and 2 reveals the differences in visible absorption between the aqueous solution and the solid phase of PXV-Br_2. It is clear that these materials absorb strongly in the visible range when in the solid state but not in aqueous solution. The chromatic properties of monomeric compounds with the bipyridinium unit have been studied and attributed to a charge-transfer interaction between the counterion and the bipyridinium ring.[12,13] The structure of a typical compound is shown here

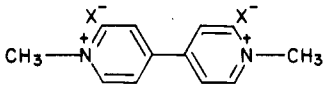

Molecular weight, water structure, and/or ionic structure of the polyelectrolytes could affect such charge-transfer (CT) interactions and account for observed differences between solutions and solids and also between monomeric and polymeric compounds.

A comparison of diffuse reflectance spectra of PXV-Cl_2, PXV-Br_2, and PXV-I_2 in Figure 2 reveals clearly differences in both the wavelength and the intensity of visible light absorption among the three solid polyelectrolytes. PXV-I_2 is the strongest absorber and also has the longest λ_{max} (see Table II). λ_{max} shifts to shorter wavelengths in PXV-Br_2 and PXV-Cl_2. It is obvious that the nature of the halide ion affects the source of chromatic activity. As indicated in Figure 3, changes in the chemical structure of the repeating unit can also have a drastic effect on visible light absorption. For example, the polyelectrolyte termed PXPE-Br_2 is essentially colorless with a λ_{max} less than 350 nm. As indicated by the chemical structures shown below, conjugation between pyridinium rings is required for chromatic properties

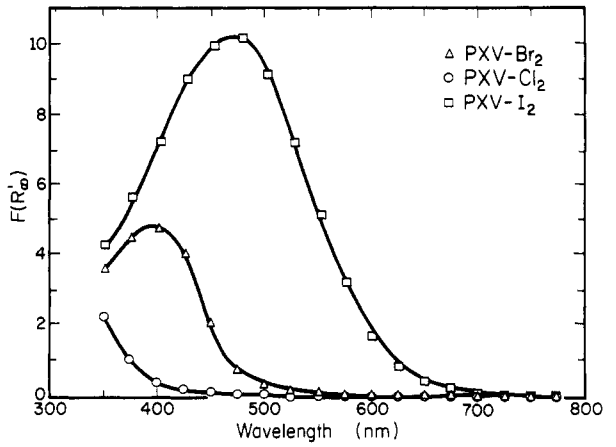

Figure 2. Plot of the remission function (see text), $F(R'_\infty)$, as a function of wavelength for solid-state samples of (□) PXV-I_2, (△) PXV-Br_2, and (○) PXV-Cl_2.

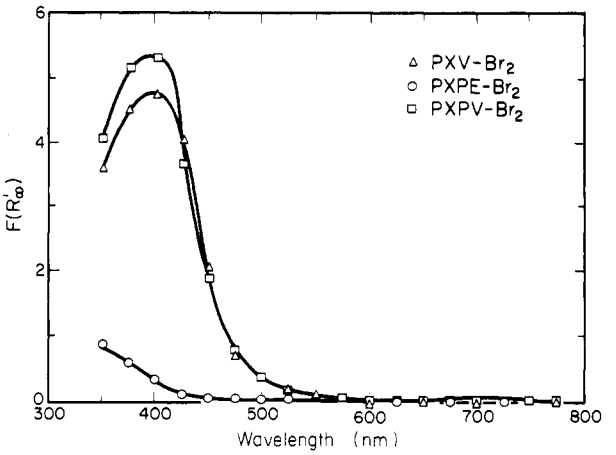

Figure 3. Diffuse reflectance spectra of PXV-Br_2, PXPE-Br_2, and PXPV-Br_2 in the solid state.

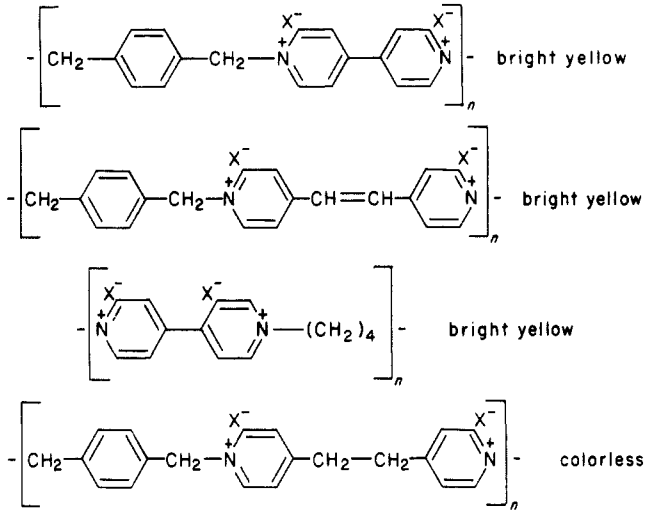

All structures shown above contain Br^- as the halide ion, which can produce strong visible light absorption providing that a conjugated bipyridinium nucleus is part of the repeating unit structure. Thus, the picture that emerges from analysis of chemical variables is the occurrence of chain-counterion CT interaction as the source of chromaticity in these polymers.

It is well-known that CT interactions involve complexation between a chemical species of high electron density and another that is electron density deficient. These molecular complexes will thus exhibit electronic absorption bands that are uncharacteristic of their components and can be understood on the basis of the molecular orbital approach of Dewar and Lepley.[16] In fact, the $\pi \rightarrow \pi^*$ transitions of the bipyridinium unit are well into the UV region (see Figure 1). Thus, the observed visible light absorption should involve CT interactions between the chain and its counterions. The existence of monomeric CT complexes involving the pyridinium or bipyridinium units as electron acceptors and halide ions as electron donors are well documented in the literature.[12,13,17-22] The absorption of visible electromagnetic radiation in PXV-Cl_2, PXV-Br_2, and PXV-I_2 results from a ground-state, ψ_N, to excited-state, ψ_E, transition. Since CT interactions are small, the relative magnitudes of transition energies can be predicted from the following equation:[16]

$$\Delta E_{CT} = I_{X^-} - A_{py^{2+}} + \text{constant} \qquad (2)$$

where ΔE_{CT} is the energy difference between ψ_N and ψ_E, I_{X^-} is the ionization potential of the halide ion (related to the energy of its highest occupied atomic orbital), and $A_{py^{2+}}$ is the electron affinity of the bipyridinium ion (related to the energy of its lowest unoccupied molecular orbital). For a given acceptor, the transition energy predicted from eq 2 should increase as the ionization potential of the halide ion increases. The ionization potential of the halides used in our study are 86, 84, and 76 kcal/mol for Cl^-, Br^-, and I^-, respectively. From the relative values of ionization potentials and eq 2, it is clear that CT energies are highest for PXV-Cl_2 and lowest for PXV-I_2, with PXV-Br_2 having intermediate values. The relative values of λ_{max} measured in this work (see Table II) for the solid polyelectrolytes are consistent with the model discussed above. Thus, absorption of shorter wavelengths by PXV-Br_2 relative to PXV-I_2 explains their being yellow vs. red.

The reflectance spectra of PXV-Br_2, PXPE-Br_2, and PXPV-Br_2 shown in Figure 3 reveal that conjugation between pyridinium rings produces a large bathochromic shift in the charge-transfer transition. This observation

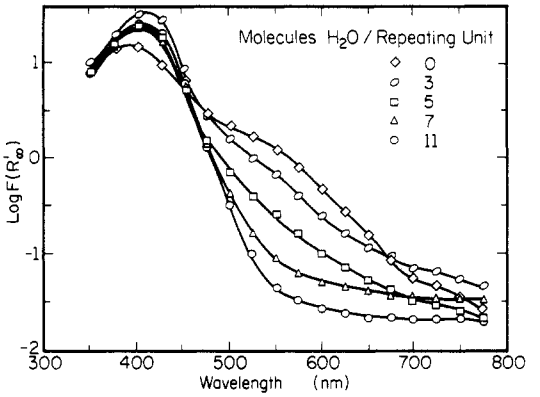

Figure 4. Diffuse reflectance spectra of PXV-Br_2 slurries showing the effect of water on chromatic properties.

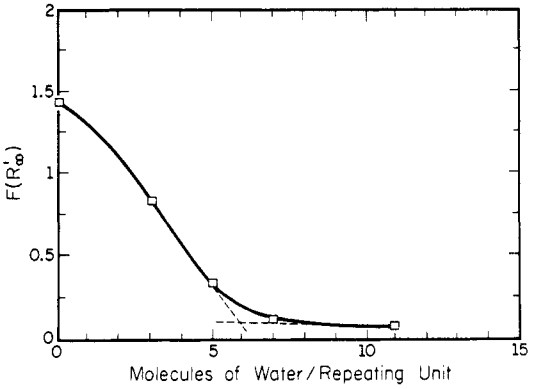

Figure 5. Plot of $F(R'_\infty)$ at 534 nm as a function of the molar ratio of water to repeating unit.

is consistent with a decrease in the charge-transfer transition energy. Following eq 2, this decrease is expected as a result of higher electron affinity in the acceptor. In the conjugated acceptor, higher electron affinity could result from delocalization of the repeating unit's divalent charge over a single π system. As stated below, the pyridinium ion has a more negative reduction potential than bipyridinium

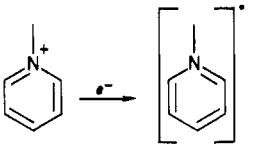

$E_{1/2}$ = -1.21 V vs. SCE

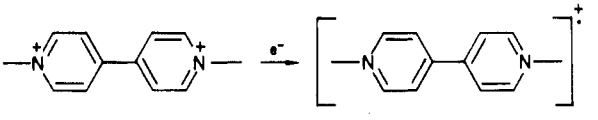

$E_{1/2}$ = -0.69 V vs. SCE

This difference supports a higher electron affinity in the conjugated acceptor of the CT pair. Accounting for the relative optical densities associated with CT interactions is a complicated issue, specially in the solid state. However, the hard/soft character of the counterions might be a useful consideration in understanding the observed optical density differences among PXV-Cl_2, PXV-Br_2, and PXV-I_2. Since the hardness of the counterions increases in the order $I^- < Br^- < Cl^-$, the strongest localized interaction between the halide ion and the nitrogen atoms may occur in PXV-Cl_2. In PXV-I_2, the more polarizable counterion may be positioned closer to the bipyridinium nucleus, resulting in a higher intensity for the CT transition. Interestingly, these ideas are supported by crystallographic

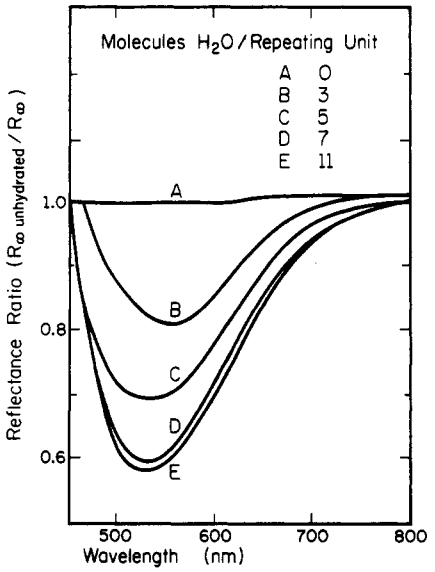

Figure 6. Ratios of reflectance in unhydrated PXV-Br_2 to reflectance in hydrated PXV-Br_2 as a function of wavelength for various water to repeating unit molar ratios.

data.[23,24] Generally speaking, the strength of the interaction vs. optical density may be controlled by factors other than just the nature of the counterion. For example, it may be affected by water structure around the macroion and its consequences on ion pair interactions as well as counterion–water interactions. The implications of our data to this particular issue are discussed below.

Figure 4 shows a family of reflectance curves for aqueous slurries of PXV-Br_2 prepared in polymerization media containing various amounts of water. The most important difference among the curves is a decreasing absorption at longer wavelengths (near 530 nm) with greater concentrations of water in the polymerization medium. In terms of color, the samples gradually transform from orange to yellow as the level of hydration increases. This observation is revealed by the curve in Figure 5 and the family of curves plotted in Figure 6. In Figure 5, the remission function for PXV-Br_2·nH_2O at the wavelength 534 nm is plotted as a function of the ratio of water molecules to monomer molecules in the polymerization medium. This curve suggests that below a critical value of water content light absorption due to the transition near 530 nm increases rapidly with further dehydration. The quantity plotted in the curves of Figure 6 is the ratio of R_∞ for an unhydrated sample to R_∞ of a series of slurries differing in level of hydration. R_∞ for an unhydrated sample is the reflectance of a slurry polymerized in the absence of water, and therefore the ratio of sample A is equal to 1. The ratio decreases with increasing levels of hydration in samples B–E, indicating progressively lower levels of absorption at the longer wavelengths in hydrated samples. Thus, the removal of water in the solid polyelectrolyte PXV-Br_2 changes its chromogenic properties; specifically, it shifts visible absorption to longer wavelengths.

Interestingly, the so-called hydrated PXV-Br_2 samples (polymerized in the presence of water) exhibited chromogenic changes with increasing temperature similar to those observed with decreasing levels of hydration. The solid bright yellow sample switches rapidly to orange upon heating and reverts back to yellow upon cooling. The color change is fast in both directions and essentially reversible. This thermochromic phenomenon is clearly revealed by Figure 7, which shows the ratio of R_∞ for a solid sample of PXV-Br_2 at three different temperatures to R_∞ of another sample at 25 °C. The temperatures were 25, 123, and 161 °C; therefore the ratio to R_∞ at 25 °C is essentially equal to 1 (prior to heating, samples were allowed to equilibrate with atmospheric moisture). The reversibility of this thermochromic change is quite evident in the $F(R'_\infty)$ plots of Figure 8. Solid PXV-I_2 also shows a similar thermochromic effect, showing an increase in absorption and wavelength upon heating. In this case, the orange-red solid formed by PXV-I_2 rapidly turns bright red upon heating.

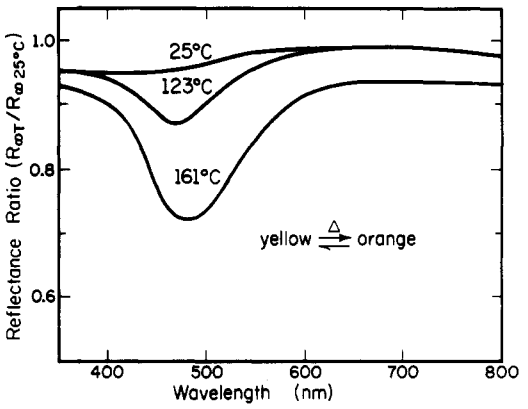

Figure 7. Ratios of reflectance in PXV-Br_2 at various temperatures to reflectance in PXV-Br_2 at 25 °C as a function of wavelength.

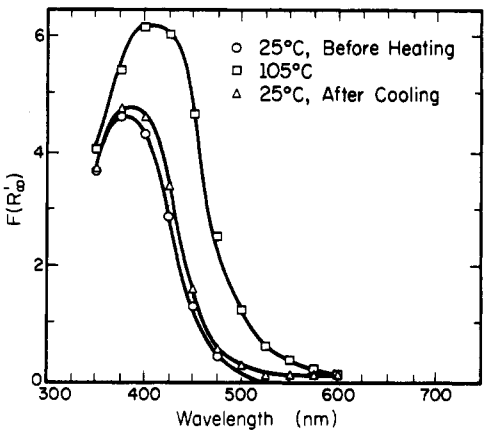

Figure 8. Diffuse reflectance spectra of PXV-Br_2 showing the reversibility of the thermochromic effect.

Since increasing temperatures and decreasing levels of hydration produce similar chromogenic effects in PXV-Br_2, we inferred that the thermochromic phenomenon was caused by dehydration and rehydration of the solid polyelectrolyte. In order to explore this problem we carried out thermogravimetric analysis (TGA) of PXV-Br_2 samples under a stream of dry nitrogen and also in the open atmosphere. As shown in Figure 9, the TGA plot suggests that dehydration occurs readily upon heating (this heating cycle would correspond to the time period during which color switching occurs). Inspection of Figure 9 (top) also reveals that rehydration does not occur upon cooling in the time span of the experiment. When cooling takes place in the open atmosphere, on the other hand, rehydration is essentially complete (see Figure 9 (bottom)). Using timed photographs in this experiment, we concluded that approximately 35 s from the time cooling started was necessary for the sample to switch from orange to yellow. On the basis of TGA data, less than 0.35 mol of H_2O per repeating unit had been readsorbed during this period of time. On the basis of the plot of Figure 5, approximately 5 mol of H_2O per repeating unit is necessary before absorbance in the range of 534 nm is lost (orange disappears). Thus, we conclude that the yellow appearance of the

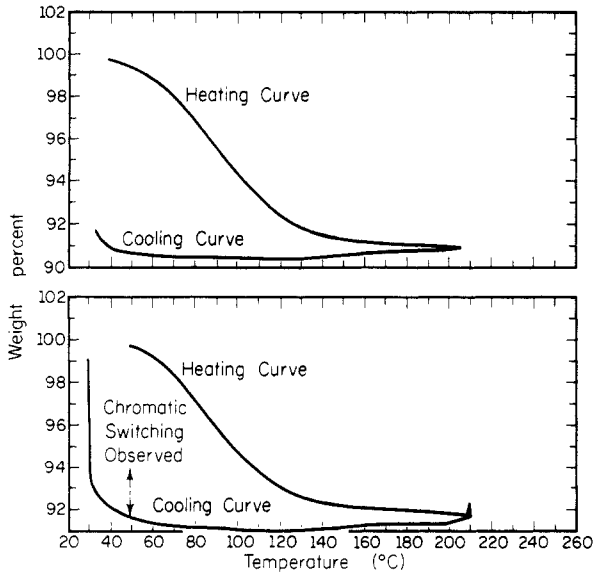

Figure 9. TGA plot of solid PXV-Br_2 recorded in a dry nitrogen atmosphere (top) and in laboratory air (bottom). The arrow indicates the point where chromatic switching was observed as revealed by a series of timed photographs.

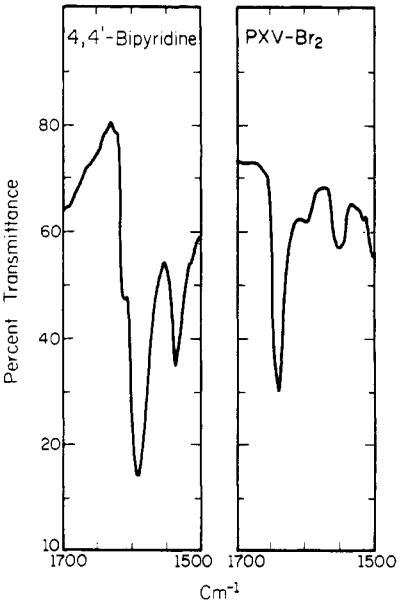

Figure 10. Infrared spectra of 4,4'-bipyridine and PXV-Br_2 in the region 1700–1500 cm^{-1}.

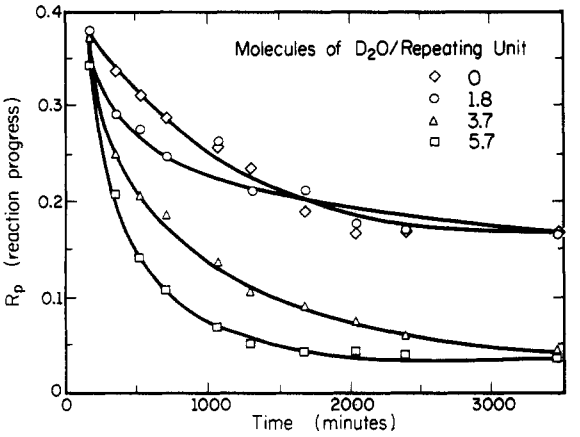

Figure 11. Kinetic curves for the polymerization of PXV-Br_2 plotted as reaction parameter (see text) vs. time for various molar ratios of water to repeating unit in the reaction medium.

sample after the small rehydration indicated by the TGA plot can be explained by rapid hydration of surface regions in the solid polyelectrolyte. In other words, the critical rehydration level for visible color switching is reached rapidly on the polymeric surface. We carried out one other experiment to verify the link between the thermochromic effect and hydration. PXV-Br_2 samples were covered with a quartz plate and heated to 150 °C. In this configuration, color switching was very slow, presumably because of the decreased dehydration rate in the presence of the quartz. Once the yellow to orange change occurred, the color remained unchanged even when samples were cooled to room temperature. As soon as the quartz plate was removed from these samples, the orange to yellow color change took place instantly. Additional evidence for the link between thermochromic phenomena and hydration level was obtained in an experiment that recorded a decreasing infrared absorption of water while a sample of PXV-Br_2 was heated to 100 °C. It is interesting to note that a visible thermochromic effect was not observed in the monomeric analogue to PXV-Br_2 synthesized in our laboratory, *N,N'*-dibenzyl-4,4'-bipyridinium dibromide. In the context of our findings this may be associated with the difficulty in producing rapid hydrating changes in the crystalline monomeric electrolyte. On the other hand, the visible thermochromic activity in the polymeric electrolyte could be based on rapid de- and rehydration of surface amorphous regions in the microstructure. In order to demonstrate unequivocally the surface nature of the observed phenomenon, one would have to carry out experiments that are beyond the scope of this investigation.

Polymerization Kinetics, Molecular Weight, and Counterion Condensation Phenomena. During the synthesis of PXV-Br_2 we noticed that the rate of color formation in the original white precipitate was strongly dependent on the amount of water present in the reaction medium. Motivated by this observation and the link between CT transitions and polyelectrolyte–water interactions, we quantified the dependence of polymerization kinetics on water concentration. The reaction progress was followed with the ratio of infrared absorbance associated with two bands, one characteristic of monomer (1590 cm^{-1}) and one characteristic of the PXV-Br_2 repeating unit (1640 cm^{-1}). The 1590-cm^{-1} band is associated with the aromatic ring stretching mode with B_{3u} symmetry in bipyridine.[25] The product absorption band at 1640 cm^{-1} is associated with the bipyridinium ion.[26,27] Spectra showing the two absorption bands used in the analysis are shown in Figure 10. We defined reaction progress by the ratio $A_{1590cm^{-1}}/(A_{1640cm^{-1}} + A_{1590cm^{-1}})$, where the A's represent infrared absorbances at 1590 or 1640 cm^{-1}. This quantity is related to the fractional concentration of monomer in the reaction medium

$$\frac{A_{1590cm^{-1}}}{A_{1640cm^{-1}} + A_{1590cm^{-1}}} = \frac{C_m}{(C_m + C_p(\kappa_p/\kappa_m))} \quad (3)$$

where C_m and C_p are concentrations of species associated with monomer and polymer, respectively, and κ_p/κ_m is the ratio of their extinction coefficients. Plots of the reaction progress parameter vs. time are shown in Figure 11 for four different water concentrations. It is clear that the rate of polymerization is strongly dependent on water concentration. With the definition of a rate parameter as $-d(R_p/dt)$ at t = 400 min, a plot of rate vs. water concentration was generated in Figure 12. When less than 2 molecules of water per monomer molecule are present, no rate increase is observed relative to the anhydrous sample. Also, the rate seems to level off when there is a high ratio of water to monomer molecules in the polymerization

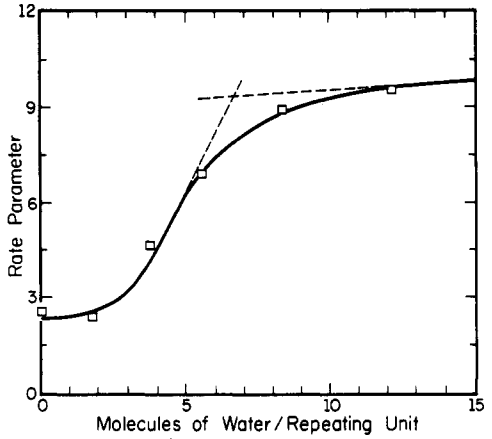

Figure 12. Plot of the rate parameter at 400 min (see text) as a function of molar ratios of water to repeating unit.

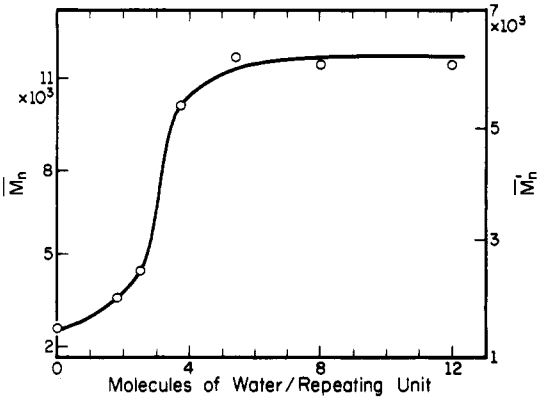

Figure 13. Plot of two different calculated values of number-average molecular weight (see text) as a function of the water to repeating unit molar ratio.

medium. An abrupt increase in polymerization rate is observed at intermediate concentrations of water. In this intermediate range there is up to a fourfold increase in reaction rate relative to the anhydrous polymerization medium. It is interesting that the large drop in polymerization rate and the appearance of light absorption near 530 nm occur in the same range of monomer to water molar ratio (compare Figures 5 and 12). We discuss below possible reasons for a link between a decreasing rate and absorption of longer wavelength visible light.

The values of reaction progress up to 165 min are essentially independent of water concentration. It is therefore possible that water availability is not a limiting factor while the colorless low molecular weight products are formed. During the initial stages of polymerization, monoalkylation of bipyridine should proceed rapidly, given its strong nucleophilic characterics. After the first quaternarization one would expect a reduced nucleophilicity as a result of reduced reactivity in the monoalkylated products. This suggestion is based on the observed reduced reactivity of pyridine when strong electron-withdrawing groups are present in the para position.[28] It is known that the Menschutkin reactions are dependent on the nature of the solvent.[29] The rates of these reactions increase with dielectric constant of the solvent, and this has been explained by the lower energy of the developing ionic character in the transition state.[29,30] However, if the dielectric constant of the solvent were the only effect involved in enhanced rate with increasing water content, one would expect a more gradual increase relative to that observed. The shape of the curve suggests that water affects the polymerization rate in a more complicated way. A possibility is that the coordination of a given number of water molecules per repeating unit is physically necessary for chain growth.

One may ask what is the physical importance of closely bound water to a nascent ionic repeating unit. Since charge sites in PXV are part of the backbone structure, a strong electrostatic repulsion would arise in the growing macroion unless effective shielding by either the counterion or water molecules can occur. This may be, in fact, a critical requirement for polymerization beyond a certain molecular weight. The shielding role of water is strongly suggested by the plot in Figure 13, which shows a significant rise in $\bar{M}_n$ of the product beyond a certain water concentration. On the other hand, leveling of $\bar{M}_n$ at high water concentration suggests that charge buildup due to the macroion's length becomes the controlling factor.

The plot in Figure 13 has two different scales of molecular weight, $\bar{M}_n$ and $\bar{M}_n'$. These two molecular weight parameters were estimated from infrared data using two different assumptions about the nature of the end groups. The $\bar{M}_n$ calculation assumes that all end groups are amino end groups. This assumption is based on the diminished reactivity of an amino group after monoalkylation. $\bar{M}_n'$ on the other hand assumes the presence of equal numbers of amino and alkyl halide end groups.

Macroions are expected to interact in different ways with their counterions; the reader is referred to the work of Oosawa for a review of this subject.[31] One interaction is the localization or condensation of counterions on individual charged groups of the macroion. In addition to these intimate ion pairs, ionic atmosphere binding can occur as well. This involves the binding of counterions over a certain volume due to the electrostatic field associated with the macroion. Counterions involved in this interaction remain mobile relative to the polymer backbone. Other counterions are considered dissociated and are therefore referred to as free counterions. The charge density of the macroion is one of the factors that determine the state of counterion binding. Other factors are counterion size and valence as well as the dielectric constant of the medium. In this context, we discuss below possible relations between counterion binding and the observed electronic transitions in PXV-Br_2.

Following Oosawa's ideas, the equilibrium between bound and free counterions in solutions of rodlike polyelectrolytes can be expressed by

$$\ln (1 - \beta)/\beta = \ln \phi(1 - \phi) + \beta Q \ln (1/\phi) \qquad (4)$$

where β is the apparent degree of dissociation of the macroion (the fraction of free counterions), ϕ is the volume concentration of the polyelectrolyte, and Q is a nondimensional quantity that determines the intensity of counterion binding

$$Q = e_0^2/\epsilon_0 kTd \qquad (5)$$

where e_0 is the electronic charge, ϵ_0 is the dielectric constant of the solution, and d is the average distance between neighboring charges on the rodlike macroion. For spherical macroions, eq 4 takes a different form; however, rodlike conformations should describe better the aromatic polyelectrolytes studied. Equation 4 predicts that at a given macroion concentration ϕ, the degree of dissociation decreases with increasing values of Q. The average macroion charge per unit chain length should be lowest in the initial stages of polymerization (low Q values) and should then increase as the average molecular weight increases with further reaction. Thus, macroions formed in the early stages of polymerization would not have the ionic structure

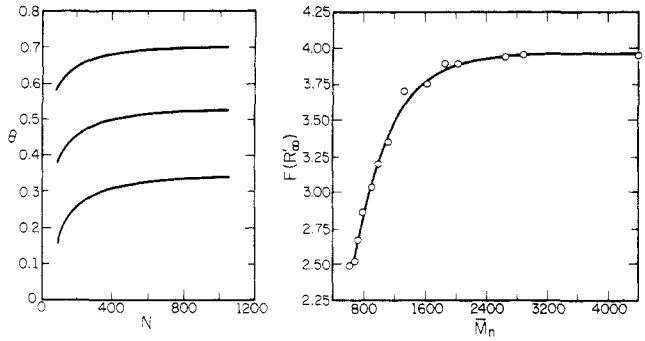

Figure 14. Theoretical plot from the work of Satoh et al.[34] for the fraction of bound counterions (θ) as a function of degree of polymerization (N). The three curves correspond to decreasing values of Q from top to bottom (left). Plot of the experimental remission function at 425 nm during the polymerization of PXV-Br_2 vs. number-average molecular weight ($\bar{M}_n$).

that favors CT interactions. That is, most counterions are free (dissociated) at first but as charge density of the growing polyion increases β decreases rapidly as new counterions produced by the reaction condense or bind to charged groups on the backbone.

We estimate Q values to be in the range 0.95–38. This is based on the dielectric constant of water and dioxane, the polymerization temperature, and an estimated average separation distance between quaternary nitrogens in PXV having a fully extended conformation. As Q values change from $Q < 1$ to $Q > 2$, the theory predicts a very large drop in the fraction of free counterions (by factors of 3 or so depending on macroion concentration). Condensed (bound) counterions should be able to participate in CT interactions due to their proximity to the electrophilic PXV backbone. Therefore, increasing values of Q as molecular weight increases could explain the transformation with time of the colorless product to a highly colored solid polyelectrolyte. In Manning's theory,[32] the degree of counterion condensation, θ, in an infinitely long chain is given by

$$\nu\theta = 1 - Q_0/Q \tag{6}$$

where ν is the valence of the counterion, and condensation occurs when $Q > Q_0$. Theoretical work by Woodbury and Ramanathan[33] predicts $Q_0 = 1$ when $\kappa L/2 \geq 1$, where κ is the Debye parameter and L is the length of the macroion. When $\kappa L/2 \ll 1$, then

$$Q_0 = \frac{\log 1/\kappa r}{\log (L/2r)} \tag{7}$$

where r is the closest distance between the counterion and the polyion. In our case $\kappa L/2$ should be in the order of 1 and Q values should be in the range 0.95–38. Thus, counterion condensation is expected at some point during the polymerization reaction.

Recent calculations by Satoh et al. have shown that the number of bound counterions increases very rapidly with molecular weight of the polyion.[34] Using their equations, the authors searched numerically for θ values that minimize free energy in the system. The prediction from their expressions is a rapid rise in θ with an increasing number of charges per macroion, N (proportional to molecular weight in our experimental polymer). After a rapid rise over a narrow range of N, θ tends to level off. Relatively large separation distances between macroion charges and bound counterions are expected in our case due to hydration. At such separations (on the order of 5 Å) the calculations of Satoh et al. predict θ to be zero below a given value of N (200 for the specific conditions used in their theoretical calculation). Interestingly, a similar trend is observed in our experiments for the increase of visible absorbance with degree of polymerization. The data we obtained is shown in Figure 14 (right), where we have plotted $F(R'_\infty)$ as a function of an estimated value of $\bar{M}_n$ from our infrared data. It is interesting that the shape of this curve resembles that of the theoretical plot by Satoh et al. for the degree of counterion condensation as a function of charges per macroion (Figure 14 (left)). On the basis of the idea that only bound counterions participate in CT interactions, $F(R'_\infty)$ should be proportional to θ. Since the number of charges per macroion is directly proportional to molecular weight, the estimated values of $\bar{M}_n$ are related to N in theoretical calculations. Thus, comparison of the two curves is consistent with our suggestion that increasing visible light absorption with average molar mass of the macroion is an optical indicator of counterion condensation.

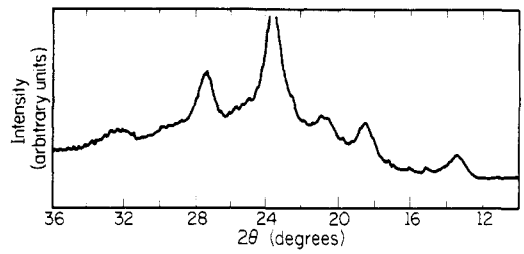

Figure 15. X-ray diffraction scan of solid PXV-Br_2.

Clearly the theoretical work discussed above applies to polyelectrolytes in solution. However, the macroion–counterion structure in the amorphous phase of the precipitated semicrystalline polyelectrolyte may reflect to some extent the ionic structure in solution. The presence of an amorphous phase in these solid polyelectrolytes is revealed by the X-ray diffraction scan of PXV-Br_2 shown in Figure 15. The curve is a superposition of diffraction peaks and an amorphous scattering halo. In amorphous regions of a solid polyelectrolyte, both localized and ionic atmosphere binding of counterions could occur. Since CT energy states require intimate counterion–macroion contact, the colorless product obtained in the initial stages of polymerization could reeflect low levels of localized counterion condensation. The yellow or orange associated with CT interactions evolves with time as polymerization proceeds, possibly indicating localized condensation and/or ionic atmosphere binding of counterions on the PXV backbone.

Condensed counterions in crystalline phases may be localized over the positively charged nitrogens not allowing strong CT interactions with the bipyridinium nucleus. In this context, it is interesting to point out that the crystalline monomeric analogue to PXV-Br_2 synthesized in our laboratory exhibits lower visible absorption relative to PXV-Br_2. The visible spectrum of this compound is shown in Figure 16, and its chemical structure is shown below:

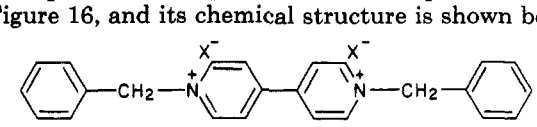

The fact that the crystalline monomeric compound does not absorb as strongly as the polymer does suggests that amorphous regions may favor the counterion–macroion structure necessary for CT interactions. In the crystalline state, the condensation of counterions may be highly localized on the positive charge. On the other hand, close approach of the counterion to the electrophilic aromatic nucleus for strong CT may occur more often in amorphous regions and perhaps only as a defect in crystalline phases.

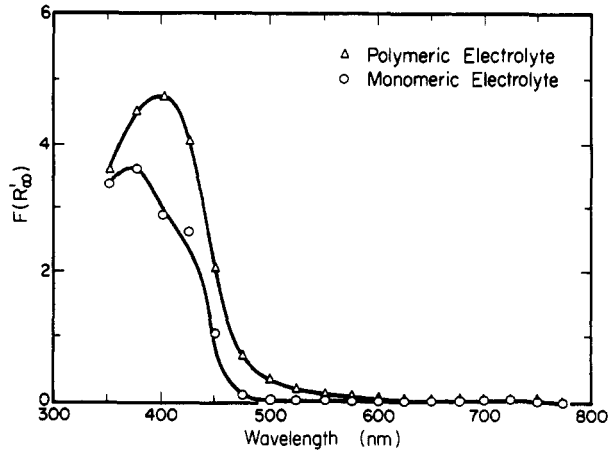

Figure 16. Diffuse reflectance spectra corresponding to PXV-Br_2 (△) and to a monomeric compound chemically analogous to PXV-Br_2 (○) (DBV-Br_2 in Table I).

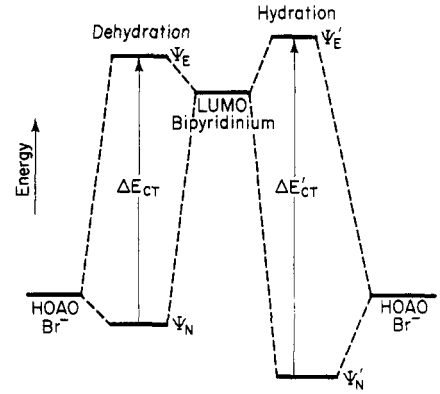

Figure 17. Schematic diagram of the relative energies associated with ground (ψ_N) and excited (ψ_E) charge-transfer states as affected by level of hydration. HOAO represents the highest occupied atomic orbital, and LUMO represents the lowest unoccupied molecular orbital.

Crystallinity of the solid polyelectrolyte should decrease as average molecular weight increases during the polymerization reaction. Thus, increasing molecular weight could be contributing to a more intense light absorption given the stronger CT activity in repeating units that are part of the amorphous phase. However, as discussed before, counterion condensation driven by increasing macroion size, and therefore charge density, is possibly the most important origin of visible light absorption. More definite conclusions on the structural nature of counterion condensation involved in CT interactions are beyond the scope of this paper. What seems clear is that macroion–counterion dissociation destroys the CT interaction, and as previously mentioned, PXV-Br_2 in aqueous solution does not exhibit visible absorption. Further evidence for dissociation vs. light absorption was provided by the preparation of the insoluble polyelectrolytic complex of PXV-Br_2 as the polycation and ionized poly(acrylic acid) as the polyanion. The stoichiometry of this complex was a 2:1 molar ratio of sodium acrylate to bipyridinium dibromide. This water-insoluble complex forms initially a bright yellow product that loses all color and becomes a white solid rapidly when exposed to a warm aqueous medium. The initial bright yellow of the complex suggests significant molecular segregation of PXV-Br_2 and sodium poly(acrylate). On the other hand, the rapid loss of color upon exposure to water indicates ionic dissociation in PXV-Br_2. It is the insoluble nature of the polyion complex that allowed us to make the observation, given that pure PXV-Br_2 partially dissolves and disperses in water. The experiment with the polyion complex provides further evidence for the idea that some type of counterion–macroion condensation is associated with the appearance of strong visible absorption.

Our study of PXV-Br_2 (thermochromic and kinetic experiments) supports the idea that water molecules become closely associated with nascent repeating units during polymerization. Thus, these macromolecules are envisioned as being sheathed by water molecules. Previous research also suggested a close association between the PXV backbone and water molecules. For example, Tsutsui and co-workers[35] found that water of hydration in minute quantities affects drastically relaxation phenomena in polymers similar to those studied here (aliphatic ionenes). One molecule of water per ionic site lowered the temperature of the main loss peak in dynamic mechanical measurements by 100 °C. Also, Ohno and co-workers[36] studied the interactions of water and these macroions by differential scanning calorimetry (DSC). On the basis of endothermic peaks observed in DSC scans, bound water was classified into three groups. The temperature at which the hydration water froze was though to be indicative of the strength of the interaction with the macroion. Water molecules bound by the strongest association froze at temperatures below −50 °C, another group of bound water froze at −30 °C. All remaining water froze at 0 °C and was considered free water. Thus, the works of Ohno and Tsutsui as well as ours suggest bound water is an important part of the structure in PXV ionenes.

The thermochromic studies reported here show that bound water affects the CT interaction. In PXV-Br_2, the electronic transition seems to shift to a higher wavelength range upon displacement of some of the bound water molecules. When this displacement is thermally induced, a reversible thermochromic effect is observed on the material's surface as long as water can evaporate. One may suggest that the observed hypsochromic shift upon hydration results from an increase in the energy separation between ψ_N and ψ_E. This concept is illustrated in the diagram of Figure 17. On the basis of our experimental results we cannot elucidate the molecular details of the hypsochromic shift. Counterion translation relative to the backbone and conformational changes induced by hydration and dehydration are both possible factors. It is also an open question whether changes in hydration are associated mostly with the polycation or with the anion. An argument presented by Kosower[18] based on the optical behavior of 1-alkylpyridinium iodide complexes could be considered to explain the observed phenomenon. This argument is related to changes in the dipole moment of the ion pairs in the ground and excited states. Kosower argued that due to the ion pairs a large dipole moment exists perpendicular to the plane of the pyridinium ring. In the excited state, however, the dipole moment decreases in magnitude and it is orthogonal to the ground-state moment. Dipole–dipole interactions can decrease the energy level of the ground state when water molecules are present. Since nuclear motions are negligible on the time scale of electronic excitation (Frank–Condon principle), no reorganization of water structure should occur at the instant of excitation. Water molecules originally oriented to maximize their interaction with ground-state structure would be unfavorably positioned in the excited state. In this context, hydration water would destabilize the excited state and stabilize the ground state. The argument by Kosower could apply to the ion pair dipole moment perpendicular to the PXV backbone. In this context, hydration and dehydration of the solid polyelectrolyte could

justify the observed hypsochromic and bathochromic shifts (see Figure 17). We emphasize, however, that the link between hydration level and chromatic switching may involve other structural factors.

In addition to the experimental results reported here, we have observed a broad range of chromatic activity in PXV's and their blends with other polymers. These observations cover essentially the entire spectrum of visible light and are certainly complex functions of molecular environment. Further work is necessary in this area, and we expect to report on it in the future.

Conclusions

Macroion-counterion charge-transfer interactions in solid poly(xylyl viologens) (PXV's) give rise to visible light absorption. The wavelength and intensity of absorption depend not only on conjugation of the cationic backbone and the nature of the counterion but also on the degree of hydration in the solid polyelectrolyte. Water molecules are closely bound to the charged repeating unit of PXV-Br_2 and therefore affect the charge-transfer states of the backbone. This is manifested by a reversible bathochromic shift during thermally induced dehydration. Counterion condensation and the presence of amorphous regions in these semicrystalline polyelectrolytes are important variables in the intensity of light absorption.

Acknowledgment. The part of this work related to synthesis of polycations received limited support from NIH Grant DE05945. We are grateful to Prof. Joseph T. Woolley of the University of Illinois for allowing us to use the spectroreflectometer in his laboratory. Finally, we acknowledge the use of equipment at the Materials Research Laboratory through a facilities grant (NSF DMR 80-20250).

Registry No. PXV-Cl_2 (SRU), 31586-24-0; PXV-Cl_2 (copolymer), 31533-65-0; PXV-Br_2 (SRU), 38815-69-9; PXV-Br_2 (copolymer), 32168-10-8; PXV-I_2 (SRU), 101979-38-8; PXV-I_2 (copolymer), 101979-40-2; PBV-Br_2 (SRU), 68842-39-7; PXPV-Br_2 (copolymer), 101979-41-3; PXPE-Br_2 (SRU), 80485-82-1; PXPE-Br_2 (copolymer), 101979-42-4; DBV-Br_2, 27768-49-6; 4,4'-bipyridine, 553-26-4; α,α'-*p*-dibromoxylene, 623-24-5; (4,4'-bipyridine)·(α,α'-*p*-dibromoxylene)·(sodium acrylate) (copolymer), 101979-43-5.

References and Notes

(1) Wenz, G.; Muller, M. A.; Schmidt, M.; Wegner, G. *Macromolecules* **1984**, *17*, 837.
(2) Patel, G. N.; Chance, R. R.; Witt, J. D. *J. Chem. Phys.* **1979**, *70*, 4387.
(3) Druy, M. A.; Seymour, R. S. *Org. Coat. Appl. Polym. Sci. Proc.* **1983**, *48*, 561.
(4) Rembaum, A.; Barmgartner, W.; Eisenberg, A. *J. Polym. Sci., Part B* **1968**, *6*, 159.
(5) Rembaum, A. *J. Macromol. Sci., Chem.* **1969**, *3*, 87.
(6) Factor A.; Heinsohn, G. E. *J. Polym. Sci., Part B* **1971**, *9*, 289.
(7) Simon, M. S.; Moore, P. T. *J. Polym. Sci., Polym. Chem. Ed.* **1975**, *13*, 1.
(8) Timofeeva, G. V.; Ivanov, V. F.; Tverskoi, V. A.; Pravednikov, A. N. *Vysokomol. Soedin., Ser. B* **1979**, *21*(9), 694.
(9) Akahoshi, H.; Toshima, S.; Itaya, K. *J. Phys. Chem.* **1981**, *85*, 818.
(10) Ohno, H.; Hosoda, N.; Tsuchida, E. *Makromol. Chem.* **1983**, *184*, 1061.
(11) Kato, M.; Oki, N.; Ohno, H.; Tsuchida, E.; Oyama, N. *Polymer* **1983**, *24*, 846.
(12) Macfarlane, A. J.; Williams, R. J. P. *J. Chem. Soc. A* **1969**, 1517.
(13) Nakahara, A.; Wang, J. H. *J. Phys. Chem.* **1963**, *67*, 496.
(14) Reich, W. S.; Rose, G. G.; Wilson, W. *J. Chem. Soc.* **1947**, 1234.
(15) Kortuem, G. *Reflectance Spectroscopy*; Springer-Verlag: New York, 1969; Chapter 4.
(16) Dewar, M. J. S.; Lepley, A. P. *J. Am. Chem. Soc.* **1961**, *83*, 4560.
(17) Kosower, E. M.; Klinedinst, P. E., Jr. *J. Am. Chem. Soc.* **1956**, *78*, 3493.
(18) Kosower, E. M. *J. Am. Chem. Soc.* **1958**, *80*, 3253.
(19) Kosower, E. M., Lindquist, L. *Tetrahedron Lett.* **1965**, *50*, 4481.
(20) Kosower, E. M. In *The Enzymes*; Boyer, P. D., Lardy, H. A., Myrback, K., Eds.; Academic: New York, 1960 Chapter 2.
(21) Foster, R. *Organic Charge-Transfer Complexes*; Academic: New York, 1969; Chapters 2 and 3.
(22) Mackay, R. A.; Landolph, J. R.; Poziomek, E. J. *J. Am. Chem. Soc.* **1971**, *93*, 5026.
(23) Russell, J. H.; Wallwork, S. C. *Acta Crystallogr., Sect. B: Struct. Crystallogr. Cryst. Chem.* **1972**, *B28*, 1527.
(24) Russell, J. H.; Wallwork, S. C. *Acta Crystallogr., Sect. B: Struct. Crystallogr. Cryst. Chem.* **1971**, B27, 2473.
(25) Gupta, V. P. *Ind. J. Pure Appl. Phys.* **1973**, *11*, 775.
(26) Cook, D. *Can. J. Chem.* **1961**, *39*, 2009.
(27) Greenwood, N. N.; Wade, K. *J. Chem. Soc.* **1960**, 1130.
(28) Arnett, E. M.; Reich, R. *J. Am. Chem. Soc.* **1980**, *102*, 5892.
(29) Abraham, M. H. *J. Chem. Soc., B* **1971**, 299.
(30) Abraham, M. H.; Grellier, P. L. *J. Chem. Soc., Perkin Trans. 2* **1976**, 1735.
(31) Oosawa, F. *Polyelectrolytes*; Marcel Dekker: New York, 1971.
(32) Manning, G. S. *J. Chem. Phys.* **1969**, *51*, 924.
(33) Ramanathan, G. V.; Woodbury, C. P. *J. Chem. Phys.* **1982**, *77*, 4133.
(34) Satoh, M.; Komiyama, J.; Iijima, T. *Macromolecules* **1985**, *18*, 1195.
(35) Tsutsui, T.; Tanaka, R.; Tanaka, T. *J. Polym. Sci., Polym. Phys. Ed.* **1976**, *14*, 2273.
(36) Ohno, H.; Shibayama, M.; Tsuchida, E. *Makromol. Chem.* **1983**, *184*, 1017.

Thermotropic Liquid Crystalline Polymers with Quasi-Rigid Chains. 1. Cyclohexyl Moieties

Maged A. Osman

Brown Boveri Research Center, CH-5405 Baden, Switzerland. *Received December 13, 1985*

ABSTRACT: Quasi-rigid polyesters and polyamides with cyclohexyl moieties in their main chains were prepared by solution polymerization. In these polymers the cyclohexyl units retained the configuration they had in the monomers. The 1,4-*trans*-cyclohexyl moieties preserved the linearity of the macromolecules, increased their flexibility, and decreased their packing density. Thus, fusible nematic polymers could be obtained. The incorporation of a mixture of *cis*- and *trans*-cyclohexyl moieties in the polymer chains also led to nematic phases although the cis isomer is nonlinear. However, the mesophase disappeared with increasing cis content.

Introduction

During the search for thermally stable polymers, the nontractable aromatic polyamides [e.g., poly(1,4-phenyleneterephthalamide)] were prepared.[1] Fibers spun from their solutions in concentrated sulfuric acid were found to have high modulus and high strength. This was attributed to the fact that these solutions possess lyotropic mesophases above a certain concentration, which lead to

0024-9297/86/2219-1824$01.50/0